Elevated copper impairs hepatic nuclear receptor function in Wilson's disease

Clavia Ruth Wooton-Kee,[1] Ajay K. Jain,[2] Martin Wagner,[3] Michael A. Grusak,[4] Milton J. Finegold,[5] Svetlana Lutsenko,[6] and David D. Moore[1]

[1]Department of Molecular and Cellular Biology, Baylor College of Medicine, Houston, Texas, USA. [2]Pediatric Gastroenterology, Hepatology and Nutrition, SSM Cardinal Glennon Children's Medical Center, Saint Louis University, St. Louis, Missouri, USA. [3]Division of Gastroenterology and Hepatology, Department of Internal Medicine, Medical University of Graz, Graz, Austria. [4]US Department of Agriculture/Agricultural Research Service (USDA-ARS) Children's Nutrition Research Center, Department of Pediatrics, and [5]Department of Pathology, Baylor College of Medicine, Houston, Texas, USA. [6]Department of Physiology, Johns Hopkins University, Baltimore, Maryland, USA.

Wilson's disease (WD) is an autosomal recessive disorder that results in accumulation of copper in the liver as a consequence of mutations in the gene encoding the copper-transporting P-type ATPase (ATP7B). WD is a chronic liver disorder, and individuals with the disease present with a variety of complications, including steatosis, cholestasis, cirrhosis, and liver failure. Similar to patients with WD, *Atp7b*$^{-/-}$ mice have markedly elevated levels of hepatic copper and liver pathology. Previous studies have demonstrated that replacement of zinc in the DNA-binding domain of the estrogen receptor (ER) with copper disrupts specific binding to DNA response elements. Here, we found decreased binding of the nuclear receptors FXR, RXR, HNF4α, and LRH-1 to promoter response elements and decreased mRNA expression of nuclear receptor target genes in *Atp7b*$^{-/-}$ mice, as well as in adult and pediatric WD patients. Excessive hepatic copper has been described in progressive familial cholestasis (PFIC), and we found that similar to individuals with WD, patients with PFIC2 or PFIC3 who have clinically elevated hepatic copper levels exhibit impaired nuclear receptor activity. Together, these data demonstrate that copper-mediated nuclear receptor dysfunction disrupts liver function in WD and potentially in other disorders associated with increased hepatic copper levels.

Introduction

Dietary copper is absorbed in the duodenum and delivered to the liver via the portal circulation, where it enters hepatocytes via the membrane copper transporter CTR1 (1). Cytosolic copper is transported into the *trans*-Golgi network via the transmembrane copper-transporting P-type ATPase ATP7 and is incorporated into ceruloplasmin, which is secreted into blood (1). In steady-state or low hepatic copper conditions, ATP7B localizes to the *trans*-Golgi compartment. Elevation of hepatic copper results in sorting of ATP7B into vesicles that traffic to the canalicular domain to promote copper excretion into bile (2, 3). Loss-of-function mutations in the *ATP7B* gene result in Wilson's disease (WD), characterized by excessive hepatic copper accumulation and a variety of symptoms including steatosis, cholestasis, cirrhosis, and liver failure, as well as neurological dysfunction (1). The *Atp7b*$^{-/-}$ mouse (4) develops hepatic copper overload by 6 weeks of age, which precedes the onset of WD symptoms (5). Transcriptional profiling at 6 weeks showed a limited number of gene expression changes that did not include alterations in redox pathways but did show a decrease in expression of genes associated with lipid metabolism (5).

Nuclear receptors consist of a variable N-terminal region, a highly conserved DNA-binding domain containing 2 zinc-binding modules that are critical for DNA-binding activity, a hinge region, and a ligand-binding domain (6). Metal replacement studies using an apo-polypeptide of the estrogen receptor (ER) α DNA-binding domain (ER-DBD) demonstrated that copper binds to the ER-DBD with greater affinity than does zinc, resulting in a disordered structure that does not bind an estrogen response element (7, 8). Since hepatic lipid metabolism is regulated by nuclear receptors and disruption may result in liver toxicity (9–12), we hypothesized that some of the metabolic symptoms in WD and in *Atp7b*$^{-/-}$ mice could be due to disrupted nuclear receptor function.

Activation of the FXR/SHP pathway inhibits production of excessive concentrations of bile acids in the liver. Bile acids activate the nuclear receptor FXR, which increases expression of short heterodimer partner (SHP), a nuclear receptor that lacks a DNA-binding domain and functions as a transcriptional repressor (13). SHP binds to another nuclear receptor, liver receptor homolog 1 (LRH-1), and recruits corepressor complexes to the promoters of genes involved in bile acid synthesis (*Cyp7a1*, *Cyp8b1*) and basolateral bile acid uptake into hepatocytes (*Ntcp),* thus decreasing both bile acid synthesis and uptake (10, 14, 15). FXR also induces the expression of canalicular transporters that excrete bile acids (via BSEP), glutathione, and glucuronidated and sulfate-conjugated compounds (via MRP2) into bile (16–18).

Since biliary secretion is a major route for copper excretion, cholestatic disorders may develop hepatic copper levels similar to those found in WD. Patients with progressive familial intrahepatic cholestasis (PFIC) 3 (MDR3 mutation, resulting in loss of biliary phospholipid excretion) (19), primary sclerosing cholangitis (PSC)

Conflict of interest: The authors have declared that no conflict of interest exists.
Submitted: September 11, 2014; **Accepted:** June 17, 2015.
Reference information: *J Clin Invest*. 2015;125(9):3449–3460. doi:10.1172/JCI78991.

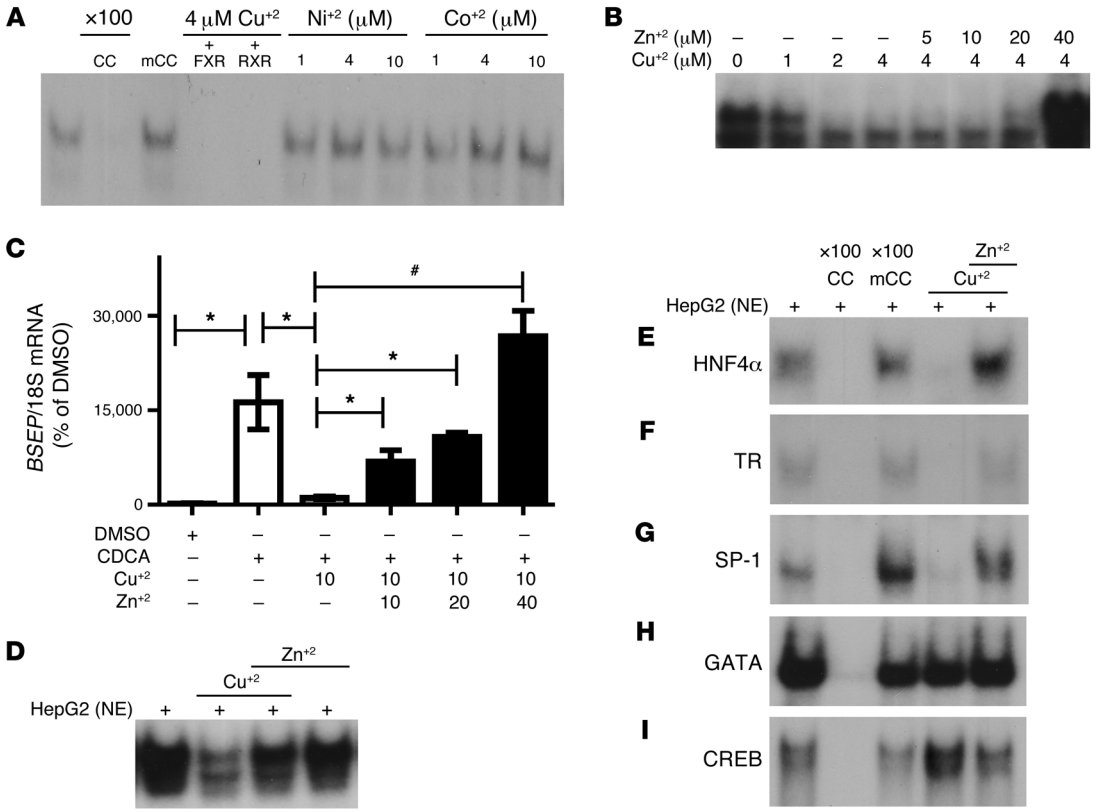

Figure 1. Copper disruption of DNA binding is reversed by zinc. (**A**) EMSA of in vitro–translated FXR and RXR with (+) or without 4 μM copper sulfate (Cu^{+2}), or 1–10 μM nickel (Ni^{+2}) or cobalt (Co^{+2}) chloride in the RXR reaction. One hundred–fold excess cold competition with WT (CC) but not mutant cold oligonucleotide (mCC). (**B**) Nuclear extracts from HepG2 cells treated with 1–4 μM Cu^{+2} or 4 μM Cu^{+2} plus 5–40 μM $ZnSO_4$ (Zn^{+2}) were incubated with a radiolabeled probe containing the FXRE on the *BSEP* promoter. (**C**) HepG2 cells were treated overnight with DMSO, 75 μM CDCA, 10 μM Cu^{+2}, and 10–40 μM Zn^{+2}, as indicated. Error bars represent the mean ± SEM. $n = 3$; $^*P < 0.05$ and $^\#P < 0.01$ by 1-way ANOVA, followed by Bonferroni's post-hoc test. (**D**) EMSA analysis of binding to the human FXRE on the *BSEP* promoter with nuclear extracts harvested from HepG2 cells treated with 10 μM Cu^{+2}, 10 μM Cu^{+2} plus 40 μM Zn^{+2}, and 40 μM Zn^{+2}. Binding of nuclear extracts from HepG2 cells treated with 10 μM Cu^{+2} or 10 μM Cu^{+2} plus 40 μM Zn^{+2} to radiolabeled oligonucleotides containing an (**E**) HNF4α, (**F**) TR, (**G**) SP1 (complex I), (**H**) GATA, or (**I**) CREB response element. NE, nuclear extract.

(20), or primary biliary cholestasis (PBC) (20) have been found to have significantly elevated hepatic copper levels and could share pathological features with WD.

We hypothesized that elevated copper levels could be associated with decreased nuclear receptor function. In accord with this prediction, we found that copper treatment strongly decreased nuclear receptor function in vitro and in cell-based studies. Nuclear receptor function was also significantly impaired in *Atp7b*$^{-/-}$ mice, WD patients, and PFIC2 and PFIC3 patients who had elevated hepatic copper levels.

Results

In vitro copper–mediated disruption of nuclear receptor function. The zinc finger containing the DBD of the nuclear receptors is highly conserved. Given the dramatic negative effect of copper on ERα binding and structure (7, 8), we performed in vitro assays to determine the direct effect of copper on metabolic nuclear receptor function. To this end, we added various metals to either FXR or RXR produced by in vitro translation. Addition of 4 μM $CuSO_4$, but not 1–10 μM nickel or cobalt, to either the FXR or RXR synthetic reaction resulted in loss of FXR:RXR binding to the *BSEP* promoter FXRE (Figure 1A). Loss of FXR:RXR binding was not due to copper-mediated changes in protein expression (Supplemental Figure 1, A and B; supplemental material available online with this article; doi:10.1172/JCI78991DS1). In a simple competition model, excess zinc would counter the effect of copper on FXR:RXR DNA binding. As expected, coincubating in vitro–translated FXR with RXR synthesized in reactions containing $CuSO_4$ plus 40 μM $ZnSO_4$ reversed the negative effect of copper on FXR:RXR binding (Figure 1B).

In HepG2 cells, CDCA-mediated induction of *BSEP* mRNA levels decreased by approximately 90% with $CuSO_4$ treatment (Figure 1C), and this was correlated with decreased FXR:RXR DNA binding in nuclear extracts (Figure 1D). However, both *BSEP* mRNA induction and nuclear extract binding were restored with $ZnSO_4$ treatment in a dose-dependent manner (Figure 1, C and D). These changes occurred in the absence of detectable changes in RXR protein levels (Supplemental Figure 1, C and D). Likewise, binding of proteins from nuclear extracts to HNF4α and thyroid hormone receptor (TR) response elements were abolished by 10 μM $CuSO_4$ treatment, which was prevented by the addition of 40 μM $ZnSO_4$ to HepG2 cell cultures (Figure 1, E and F).

To determine whether copper could affect DNA binding of other zinc-containing transcription factors, we examined the

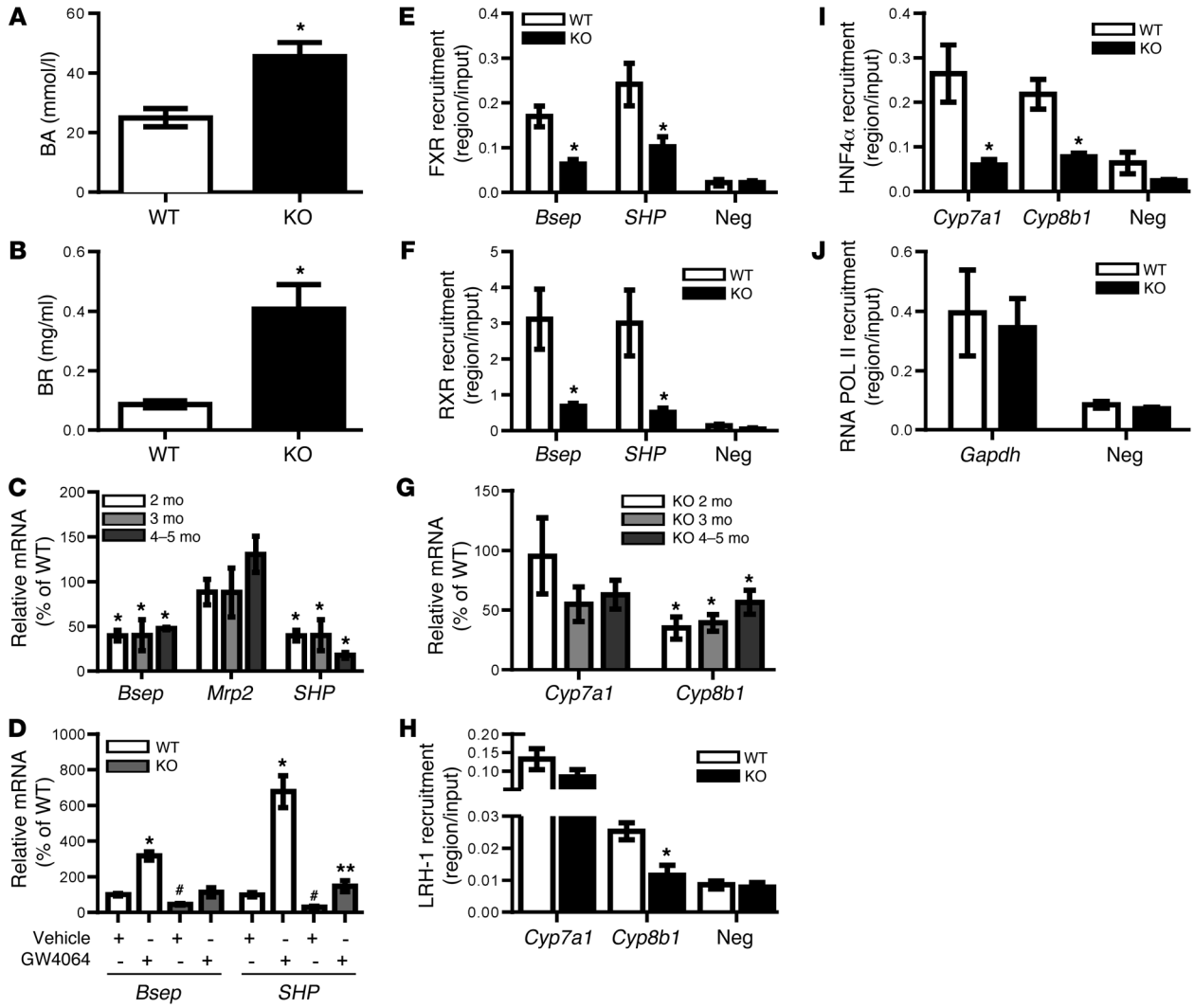

Figure 2. Nuclear receptor activity in *Atp7b*$^{-/-}$ mice. (**A**) Serum bile acid (BA) and (**B**) bilirubin (BR) levels were measured in 3-month-old WT and *Atp7b*$^{-/-}$ mice. (**C** and **G**) *Bsep*, *Mrp2*, *SHP*, *Cyp7a1*, and *Cyp8b1* mRNA expression levels were measured by real-time PCR for WT and *Atp7b*$^{-/-}$ mice at 2, 3, and 4–5 months of age. The A*tp7b*$^{-/-}$ target gene expression level is a percentage of that of the age-matched WT control. (**D**) Mice were given DMSO or 50 mg/kg BW GW4064 four hours prior to harvesting livers for analysis of *Bsep* and *SHP* mRNA levels. (**E**, **F**, and **H**–**J**) ChIP was performed using formaldehyde–cross-linked and purified nuclei and FXR, RXR, HNF4α, LRH-1, and RNA Pol II antibodies as indicated. The response elements on each promoter were amplified by real-time PCR and normalized to input. Primers for a gene desert region were used as a negative control (Neg). Error bars represent the mean ± SEM. *$P < 0.05$ by Student's *t* test (**A** and **B**, $n = 6$–12 samples; **E** and **F** and **H** and **I**, $n = 4$ samples); *$P < 0.05$ by 1-way ANOVA, followed by Bonferroni's post-hoc test (**C** and **G**, $n = 4$–6 samples); $P < 0.05$ by 2-way ANOVA, followed by Bonferroni's post-hoc test (*WT versus KO GW4064 treatment, #WT versus KO vehicle, and **KO vehicle versus GW4064) (**D**, $n = 4$–6 samples).

Cys_2His_2 transcription factor SP1 and the Cys_4 transcription factor GATA4. Like the nuclear receptors, SP1 DNA binding was lost in the copper-treated cells and restored by cotreatment of HepG2 cells with 40 μM $ZnSO_4$ (Figure 1G); however, GATA binding was unchanged (Figure 1H). Binding of nuclear extracts to a radiolabeled probe containing the leucine zipper transcription factor CREB consensus element was not decreased with metal treatment (Figure 1I). Thus, the detrimental effects of copper occur in a protein-specific manner.

Atp7b$^{-/-}$ *mice have disrupted hepatic nuclear receptor function and expression of metabolic target gene expression.* At 6 weeks of age, *Atp7b*$^{-/-}$ mice have increased serum alanine aminotransferase (ALT) and hepatic copper levels, which precedes overt liver pathology (5), and we confirmed these results (Supplemental Figure 2). We found 1.8-fold and 5-fold increases in serum bile acid and bilirubin levels in 3-month-old mice (Figure 2, A and B) but no changes in the total hepatic bile acid pool size (data not shown), which suggested disrupted hepatic bile acid metabolism. Therefore, we measured the mRNA levels of hepatic FXR target genes. In 2- to 3-month-old mice, *Bsep* and *SHP* mRNA expression was decreased to 40% of control levels, and *SHP* was decreased further to 20% of WT control levels at 5 months of age; however, *Mrp2* mRNA expression was unchanged (Figure 2C). Despite changes in FXR:RXR basal activity, *Atp7b*$^{-/-}$ mice showed a residual response to the potent FXR ligand GW4064 (4.9-fold increase, $P = 0.02$ for *SHP* mRNA expression); however, GW4064-induced expression levels of *Bsep* and *SHP* mRNA in *Atp7b*$^{-/-}$ mice were much lower than those detected in WT mice (Figure 2D).

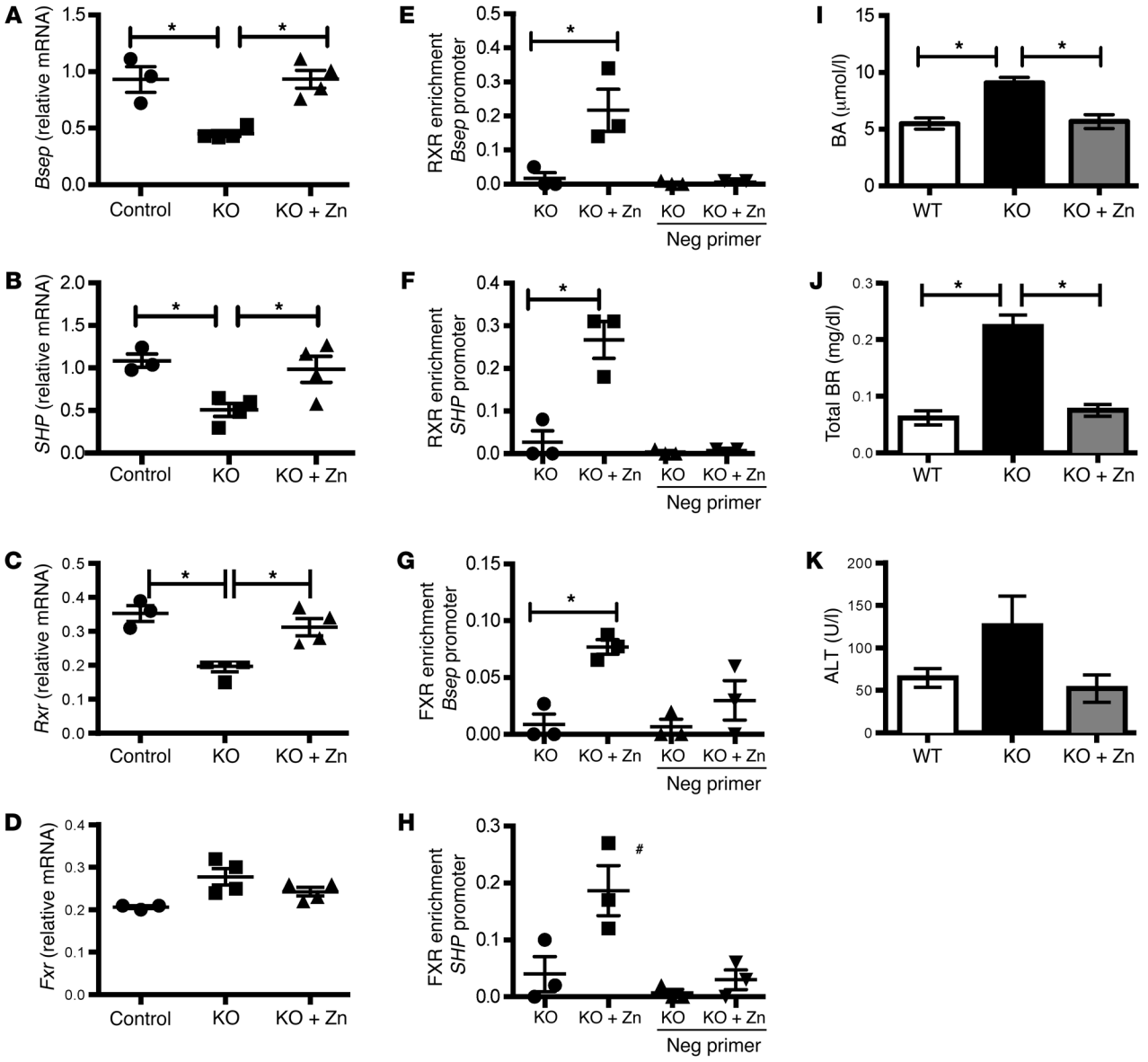

Figure 3. In vivo effects of zinc therapy on nuclear receptor activity in *Atp7b*$^{-/-}$ mice. (**A**) *Bsep*, (**B**) *SHP*, (**C**) *Rxr*, and (**D**) *Fxr* mRNA expression was measured by real-time PCR for WT and *Atp7b*$^{-/-}$ (KO mice on a chow diet or on a diet supplemented with 1,000 ppm zinc acetate). ChIP was performed using formaldehyde–cross-linked and purified nuclei and (**E** and **F**) RXR or (**G** and **H**) FXR antibodies. The response elements on each promoter were amplified by real-time PCR and normalized to input. Primers for a gene desert region of chromosome 6 were used as a negative control. Serum (**I**) bile acids, (**J**) bilirubin, and (**K**) ALT levels were measured for WT, KO, and zinc-supplemented KO (KO + Zn)animals. Data represent the mean ± SEM. $^{*}P < 0.05$ by 1-way ANOVA, followed by Sidek's post-hoc test (**A**–**C**, $n = 3$ samples; **I** and **J**, $n = 3$–6 samples). $^{*}P < 0.05$ by Student's *t* test (**E**–**G**, $n = 3$ samples); $^{\#}P = 0.052$ by Student's *t* test (**H**, $n = 3$ samples).

ChIP analysis revealed that FXR and RXR binding to the *Bsep* and *SHP* promoters was reduced by 70% (FXR) and 80% (RXR) in *Atp7b*$^{-/-}$ livers relative to WT control livers at 2 to 5 months of age (Figure 2, E and F); binding was not further decreased between 2 and 5 months of age (data not shown). *Rxr* mRNA levels were decreased, but changes in *Fxr* mRNA levels were detected only at 5 months of age (Supplemental Figure 3A), in contrast to the in vitro data, which did not show changes in RXR protein expression in samples treated with copper. Chronic copper accumulation in the *Atp7b*$^{-/-}$ mouse liver may result in activation of hepatic stellate and Kupffer cells and pathways, such as the inflammatory pathway, that decrease RXR expression (21–25).

LRH-1 and HNF4α are orphan nuclear receptors that are essential for the regulation of bile acid synthetic genes, such as *Cyp7a1* and *Cyp8b1*. *Cyp7a1* mRNA expression levels trended lower in *Atp7b*$^{-/-}$ mice (45% decrease, $P = 0.12$ at 3 months of age and 38% decrease, $P = 0.14$ at 5 months of age) (Figure 2G). LRH-1 binding to the *Cyp7a1* promoter was unchanged (Figure 2H), whereas HNF4α binding was significantly decreased in these mice at 5 months of age (Figure 2I). *Cyp8b1* mRNA expression levels decreased by 65% in the *Atp7b*$^{-/-}$ mice at 2 to 3 months of age and by 44% at 5 months

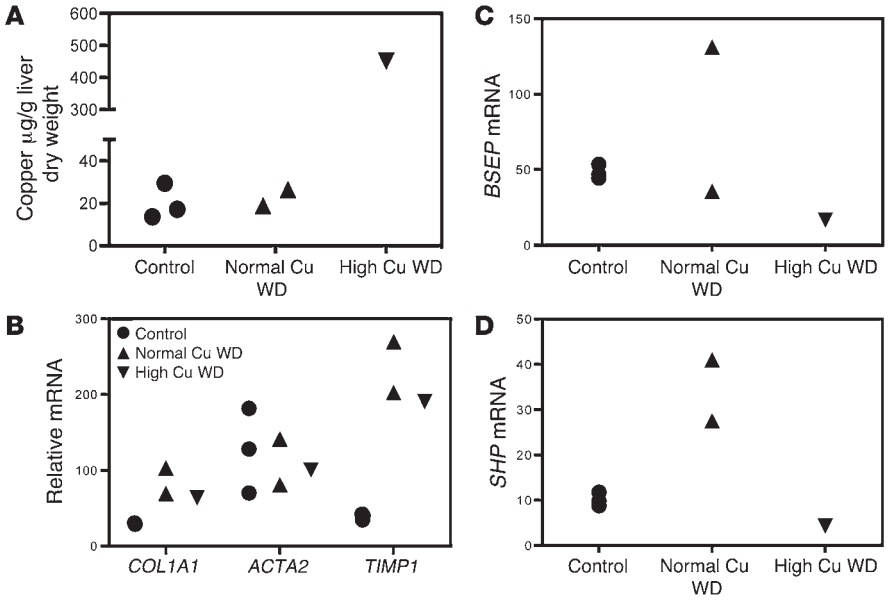

Figure 4. Characterization of adult WD patients. (**A**) Liver dry weight (μg/g) was determined by ICP-OES. Real-time PCR for mRNA expression of (**B**) *COL1A1*, *ACTA2*, *TIMP1*, (**C**) *BSEP*, and (**D**) *SHP* from NDRI adult liver tissue samples. (**B**–**D**) Samples are grouped according to the degree of hepatic copper levels: control (non–liver disease samples), normal Cu WD (WD samples without elevated hepatic copper levels), and high Cu WD (WD samples with hepatic copper levels that meet WD criteria). For each experiment, samples were measured in duplicate and the average plotted for the individual sample. Each experiment was performed 3 times, and all graphs are representative of 3 separate experiments.

of age relative to WT levels (Figure 2G). As with *Cyp7a1*, recruitment of HNF4α to the *Cyp8b1* promoter decreased by approximately 60% at 5 months of age in the *Atp7b*$^{-/-}$ mice (Figure 2I). There was a 60% (P = 0.057) downward trend in LRH-1 binding to the *Cyp8b1* promoter in these mice at 2 months of age (data not shown) and a 55% decrease by 5 months of age (Figure 2H). Binding of RNA Pol II to the *Gapdh* promoter was the same in both WT and *Atp7b*$^{-/-}$ livers (Figure 2J). No changes in *Lrh1* or *Hnf4a* mRNA expression were detected in *Atp7b*$^{-/-}$ mice at 2 to 5 months of age (Supplemental Figure 3A). Other LRH-1 and HNF4α target genes involved in hepatic metabolism (*Ntcp*, basolateral transport) and biliary cholesterol transport (*AbcG5* and *AbcG8*), as well as the TR and PPARα target genes *Spot14* and *G6Pase*, had decreased expression in the *Atp7b*$^{-/-}$ mice at 2 to 5 months of age (Supplemental Figure 4).

A zinc-enriched diet prevents decreased nuclear receptor function. WD patients are treated with zinc following successful chelation therapy (26–30). Zinc therapy is thought to decrease copper load by competing with copper for absorption in the small intestine (26, 27, 31). Given the protective effect of zinc on nuclear receptor activity in vitro, we tested whether zinc had a protective effect on hepatic nuclear receptors in *Atp7b*$^{-/-}$ mice. To maximize zinc exposure prior to significant increases in hepatic copper levels, mice in mating cages were given a chow diet enriched with zinc acetate (1,000 ppm), and the diet was maintained after weaning until the mice were 2 months of age. We then measured target gene expression and nuclear receptor binding. Control littermate mice given the zinc-enriched diet did not have significant changes in target gene expression or nuclear receptor binding relative to control mice given a regular chow diet (data not shown). The zinc-supplemented *Atp7b*$^{-/-}$ mice had significant increases in *Bsep*, *SHP*, and *Rxr* mRNA expression levels, whereas *Fxr* mRNA expression levels were unchanged in the KOs fed regular or zinc-supplemented chow relative to levels in WT controls (Figure 3, A–D). In accord with the mRNA expression levels, ChIP showed that zinc supplementation increased RXR binding to the *Bsep* and *SHP* promoters and FXR binding to the *Bsep* promoter (Figure 3, E–G), and there was an upward trend in binding of FXR to the *SHP* promoter (P = 0.052) (Figure 3H). Modest, yet significant, improvements were also observed in *Ntcp* and *Cyp8b1* mRNA expression levels (Supplemental Figure 5). Zinc treatment also reduced serum bile acid and bilirubin levels and restored ALT to WT levels (Figure 3, I–K). Taken together, our findings show that zinc treatment prevented significant disruption of nuclear receptor function and improved serum markers of liver function.

WD patients with elevated hepatic copper have disrupted metabolic nuclear receptor signaling. Aside from findings of decreased biliary copper excretion (32, 33) without pathological changes in total bile acids (34), there are a limited number of studies regarding bile acid metabolism in WD patients. To address whether WD patients exhibit changes similar to those seen in the WD mouse model, we measured nuclear receptor target gene mRNA expression and activity in adult hepatic autopsy samples obtained from the National Disease Research Interchange (NDRI). We did not have access to data on disease pathology or severity, so we measured copper concentrations in the samples by inductively coupled plasma optical emission spectrometry (ICP-OES). Surprisingly, only 1 WD sample had hepatic copper levels in the WD diagnostic criteria range (451 μg/g liver dry weight vs. 25 μg/g liver dry weight) (Figure 4A). Despite this discrepancy, all WD samples had changes in hepatic markers of liver injury and hepatic stellate cell activation, such as increased mRNA of the fibrogenic marker tissue inhibitors of matrix metalloproteinase 1 (*TIMP1*) (Figure 4B). Collagen 1A1 (*COL1A1*) mRNA expression was slightly higher in all WD samples (Figure 4B); however, α smooth muscle actin (α-SMA, *ACTA2*) mRNA, another marker of hepatic stellate cell activation and fibrogenesis, was not changed in the WD samples (Figure 4B). Overall, this may reflect a more advanced stage of cirrhotic liver disease, since α-SMA has been shown to increase with initial stellate cell activation and decrease with prolonged activity (35).

For further analysis, the WD samples were grouped according to copper levels: normal copper (Cu) WD and high Cu WD. The high Cu WD sample had the lowest *BSEP* and *SHP* mRNA expres-

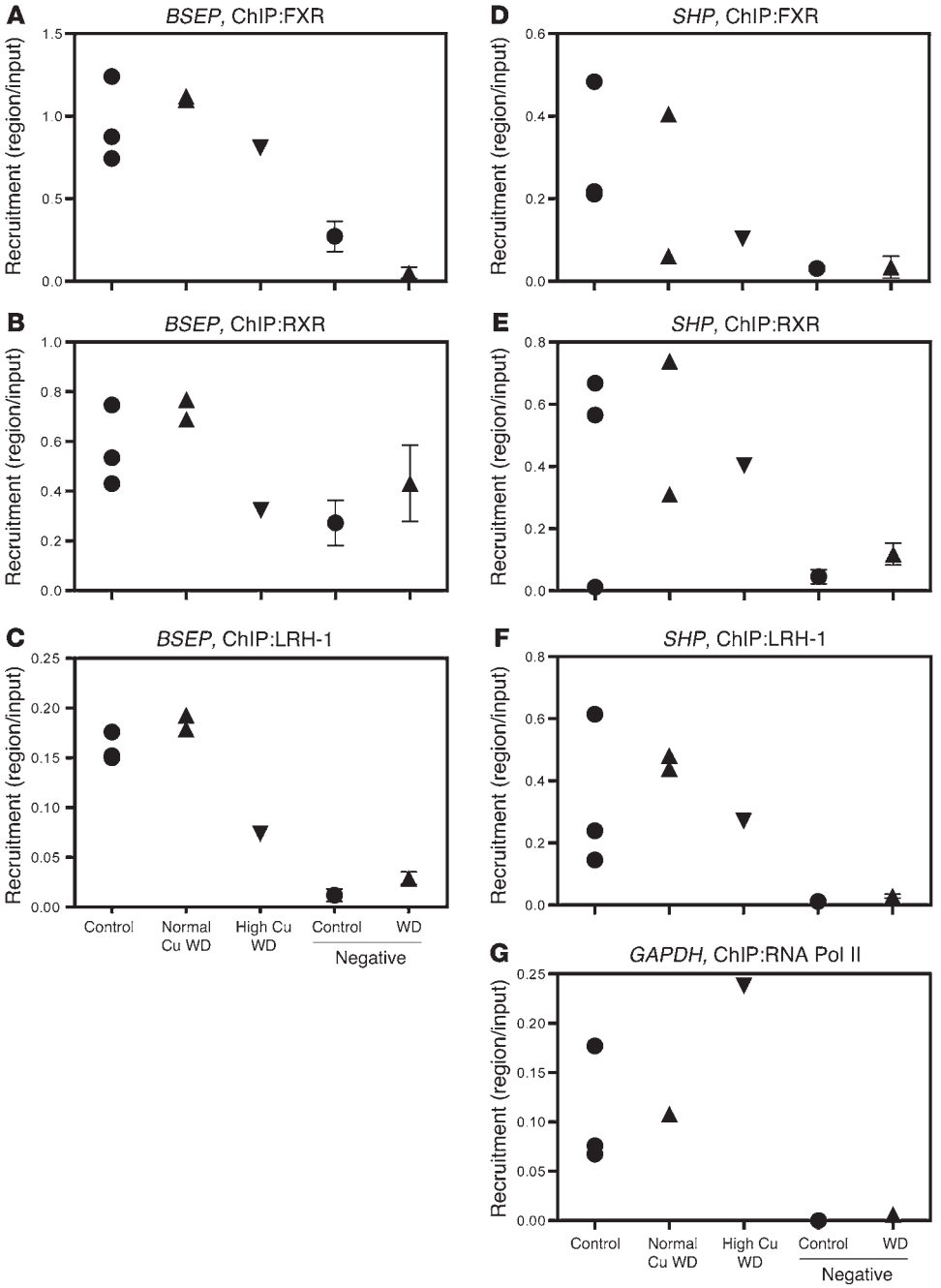

Figure 5. ChIP analysis of adult control and WD samples. ChIP was performed with (**A** and **D**) FXR, (**B** and **E**) RXR, (**C** and **F**) LRH-1, and (**G**) RNA Pol II. The response elements on each promoter were amplified by real-time PCR and normalized to input. Primers designed for a gene desert region of chromosome 12 were used as a negative control. Samples are grouped according to the degree of hepatic copper levels: control (non–liver disease samples), normal Cu WD (WD tissue samples from patients without elevated hepatic copper levels), and high Cu WD (WD tissue samples from patients with hepatic copper levels meeting WD criteria). For each experiment, samples were measured in duplicate and the average plotted for the individual sample. Each experiment was performed 3 times, and graphs are representative of 3 separate experiments.

sion levels (Figure 4, C and D) and binding of FXR and RXR to the *BSEP* promoter (Figure 5, A and B). Binding of LRH-1 to the *BSEP* promoter was also lowest in the high Cu WD sample group (Figure 5C). Similarly, binding of FXR, RXR, and LRH-1 to the *SHP* promoter was lowest in the high Cu WD sample; however, binding was in the range of the control samples (Figure 5, D–F). RNA Pol II binding to a positive control primer for *GAPDH* was similar among the groups (Figure 5G). *CYP7a1* and *CYP8b1* mRNA expression levels were not decreased in the WD samples, and LRH-1 and HNF4α binding was in the range of the control and normal Cu WD samples (Supplemental Figure 6). CYP7a1 has a well-defined circadian rhythm (36, 37), and CYP7A1 expression is negatively regulated by miR-122a and miR-422a (38). This finding may reflect differences in *CYP7a1* mRNA stability and/or posttranslational mechanisms in the *Atp7b*$^{-/-}$ mouse versus the those in fibrotic WD human samples. Similar to *Atp7b*$^{-/-}$ mice, patients with WD do not have significant changes in mRNA expression of *LRH1*, *HNF4A*, or *FXR*; however, *RXR* mRNA was increased in both groups of patients with WD (Supplemental Figure 3B). Despite these differences in RXR expression, both KO mice and WD patients with elevated hepatic copper levels had decreased recruitment of RXR in binding assays.

Pediatric WD and PFIC patients have elevated hepatic copper levels and disrupted nuclear receptor function. We also obtained several pediatric biopsy samples from controls (noncholestatic patients with normal hepatic copper levels); from a WD patient treated with the metal chelation therapy trientine (WD/trientine) and given a

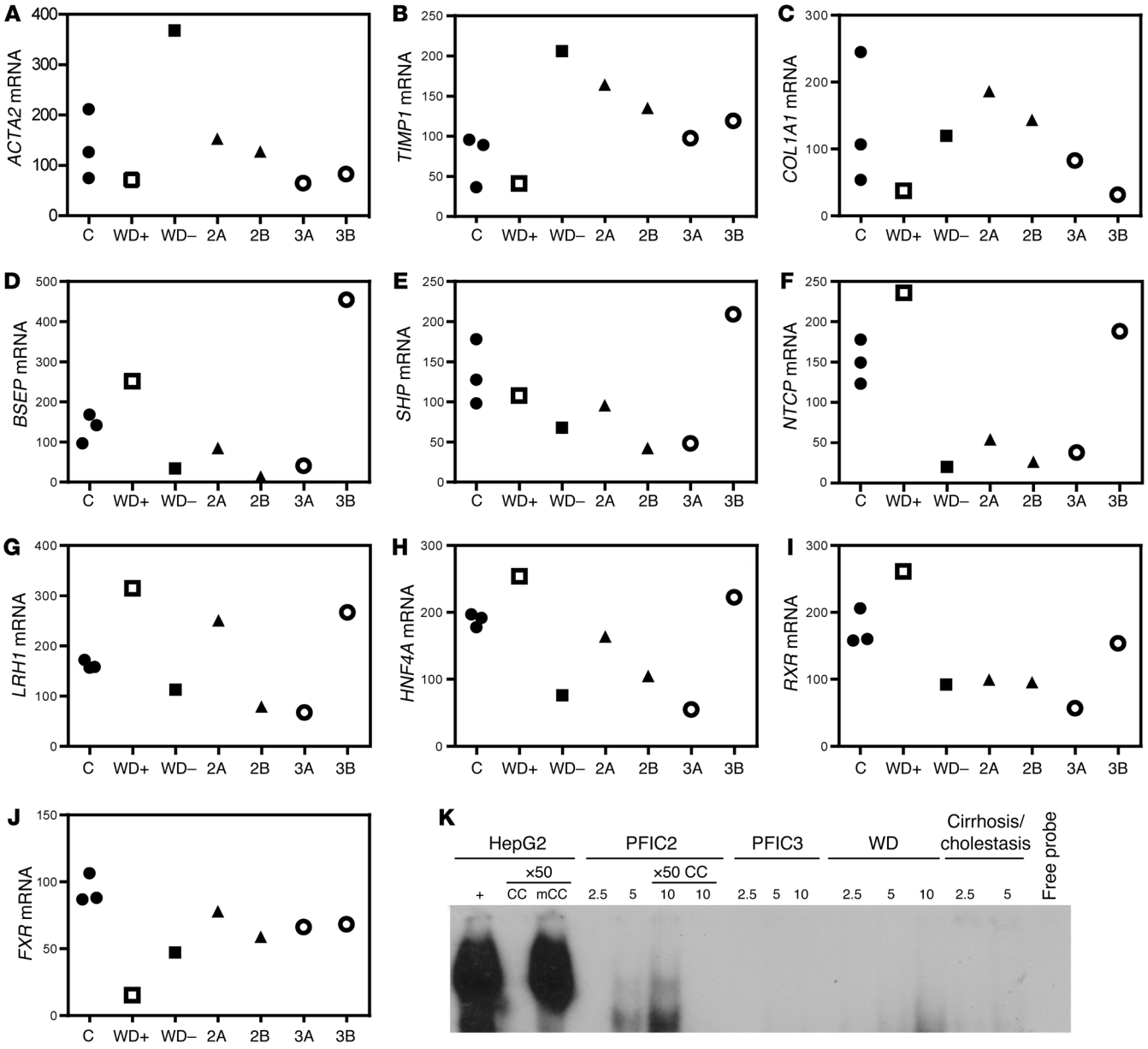

Figure 6. Pediatric cholestasis and copper-mediated effects on nuclear receptors. (**A**–**J**) Real-time PCR was performed to measure *COL1A1*, *ACTA2*, *TIMP1*, *BSEP*, *SHP*, *NTCP*, *LRH1*, *HNF4A*, *RXR*, and *FXR* mRNA in pediatric liver biopsy samples. mRNA levels in tissue samples from controls (C, denoting pediatric patients with normal hepatic copper levels), WD/trientine patients (WD+), WD/no trientine patients (WD–), PFIC2 patients A and B (2A, 2B), and PFIC3 patients A and B (3A, 3B). For each experiment, samples were measured in duplicate and the average plotted for the individual sample. Each experiment was performed 3 times, and graphs are representative of 3 separate experiments. In panels **A**–**J**, target gene mRNA expression was normalized to 18S mRNA expression. (**K**) EMSA analysis of binding to a radiolabeled probe containing an FXRE on the *BSEP* promoter with nuclear extracts harvested from HepG2 cells or from patients with PFIC2, PFIC3, WD, or cirrhosis or cholestasis. Fifty-fold excess of cold competition with WT (CC), but not mCC, demonstrated specific and nonspecific binding.

low-copper diet; and from a newly diagnosed WD patient who was not treated with trientine chelation therapy (WD/no trientine). To determine overall fibrotic changes in the liver, we measured *COL1A1*, *ACTA2*, and *TIMP1* mRNA and found that *ACTA2* and *TIMP1* levels were approximately 3-fold and 2-fold higher in the WD/no trientine group than the average levels in the control samples, which the WD/trientine sample overlapped (Figure 6, A and B); however, *COL1A1* mRNA expression levels were similar in both WD groups (Figure 6C). The liver sample from the WD/no trientine patient had lower *BSEP*, *SHP*, and *NTCP* mRNA expression levels than did the liver sample from the WD/trientine patient (Figure 6, D–F). The WD/no trientine patient had decreased *LRH1*, *HNF4A*, *RXR*, and *FXR* mRNA expression levels (Figure 6, G–J), and *FXR* mRNA expression levels were lower than those in the control samples from the WD/trientine patient. *RXR* mRNA expression patterns in the pediatric WD/no trientine patient were similar to those in the *Atp7b*$^{-/-}$ mice, which may point to a central importance of RXR in the dysregulation of nuclear receptor signaling in WD.

We expanded upon the studies of others (19), who demonstrated elevated hepatic copper levels in cholestatic liver disease, and obtained liver biopsy samples from 2 patients with PFIC3 (MDR3 mutation) and from 2 patients with PFIC2 (BSEP mutation). Similar to the samples from adult WD and pediatric WD/no trientine patients, both PFIC2 and PFIC3 samples had elevated mRNA expression of *TIMP1*; however, *COL1A1* and *ACTA2* mRNA expression overlapped that of controls (Figure 6, A–C). PFIC3 patient A had hepatic copper levels that were well within the WD criteria (1136 μg/g liver dry weight) and decreased expression levels of *LRH1*, *HNF4A*, *RXR*, *BSEP*, *SHP*, and *NTCP* mRNA that were similar to those detected in the WD/no trientine patient (Figure 6, D–I). For PFIC3 patient B, rhodanine staining demonstrated significant copper staining within zone 1 hepatocytes, as was seen in a WD patient (Supplemental Figure 7), but nuclear receptor and target gene mRNA expression overlapped that of the control pediatric samples (Figure 6, D–F). Hepatic copper levels in PFIC2 patient A were elevated (177 μg/g liver dry weight) but slightly below typical WD levels. Data regarding copper concentrations were not available for PFIC2 patient B, due to the small sample size. Both PFIC2 patients had a downward trend in mRNA expression of *BSEP*, *SHP*, and *NTCP* (Figure 6, D–F). As in the pediatric WD/no trientine patient, *LRH1* and *HNF4A* mRNA levels were decreased in PFIC2 patient B and PFIC3 patient A (Figure 6, G and H). All PFIC patients had *RXR* and *FXR* mRNA levels overlapping those of WD/no trientine patients (Figure 6, I and J), and hence lower than control mRNA expression levels.

We confirmed decreased FXR:RXR binding in samples from PFIC2 patient A, PFIC3 patient A, an additional WD patient (865 μg copper/g liver dry weight), and a patient with cholestasis and cirrhosis (727 μg copper/g liver dry weight) using EMSA analysis. Because of the limited sample amounts for each patient, we were unable to perform Western blot or ChIP assays. Nuclear extracts from HepG2 cells were used as a positive control for binding of FXR:RXR to the FXR response element (FXRE) of the human *BSEP* promoter. Binding in the PFIC2 sample was reduced, yet specific, to the FXRE (Figure 6K). No specific binding was found in the nuclear extracts from the other pediatric nuclear extract samples analyzed (Figure 6K). To the best of our knowledge, these studies are the first to describe changes in nuclear receptor function in WD and to correlate changes in nuclear receptor function with hepatic copper levels in patients with cholestasis.

Discussion

Copper is an essential trace element that serves as a cofactor for many metabolic enzymes, such as cytochrome c oxidase and ceruloplasmin, but excessive copper levels can result in cell stress and cell death. While much is known about the role of excessive copper in the generation of redox-oxidative stress, copper-mediated disruption of nuclear receptor signaling in vivo has not been described. Herein, we describe changes in hepatic metabolic nuclear receptor activity in the livers of the *Atp7b*$^{-/-}$ WD mouse model and of patients with WD and PFIC.

Studies using mass spectrometry electrospray ionization (MS-ESI) confirmed a bicoordinate interaction of the ER with copper (39) and strong copper-induced alterations in protein structure (8). In agreement with the ERα studies, in vitro translation of either FXR or RXR in the presence of copper resulted in loss of FXR:RXR binding to an FXRE. This was not due to changes in the efficacy of the in vitro translation reaction (data not shown) and occurred when a previously generated FXR:RXR complex was incubated overnight at 4°C with copper (data not shown). Strong impairment of nuclear receptor function was also observed in HepG2 cells treated with copper, as shown by inhibition in the CDCA-mediated induction of *BSEP* mRNA expression and loss of specific DNA binding by FXR:RXR, HNF4α, or TRα:RXR. These copper-mediated decreases in transcription factor function extended to the Cys2His2 transcription factor SP-1, but not the Cys4 transcription factor GATA4 or the leucine zipper transcription factor CREB. Differences in zinc finger coordination among different zinc-containing transcription factors may result in a spectrum of susceptibility to copper interaction with the zinc finger proteins.

In agreement with previous studies, we found that *Atp7b*$^{-/-}$ mice at 3 months of age had elevated hepatic copper levels that were within the WD diagnostic criteria, elevated serum ALT, as well as elevated bilirubin and bile acid levels. We measured the activity of nuclear receptors involved in bile acid metabolism and transport, as well as other metabolic targets, and found that mRNA expression of FXR:RXR targets was decreased in these mice at 2 months of age, which precedes full-blown liver pathology (5, 40). *Bsep* and *SHP* mRNA were decreased in *Atp7b*$^{-/-}$ mice, and the recruitment of FXR and RXR to the *Bsep* and *SHP* promoters was strongly decreased. RXR expression was decreased in these mice beginning at 2 months of age, whereas FXR expression was not changed until 5 months of age. While the mechanism for RXR reduction is unclear, decreased RXR could contribute to reduced binding of FXR:RXR to the response elements on the *Bsep* and *SHP* promoters.

WD does not result in elevated intestinal copper levels, therefore, copper-mediated effects on nuclear receptor activity should not be manifest in the intestine of *Atp7b*$^{-/-}$ animals. GW4064 treatment induced duodenal *Fgf15* mRNA expression by approximately 8-fold in both WT and KO animals (data not shown). Studies in intestine- or liver-specific *Fxr*-KO mice demonstrated that intestinal activation of FGF15 can activate *SHP* mRNA expression in the absence of hepatic FXR expression (15). Since FGF15 signaling is present in the *Atp7b*$^{-/-}$ animals, activation of intestinal FGF15 expression may contribute to the GW4064-mediated activation of *SHP* mRNA expression.

Despite a decrease in *Bsep* mRNA expression, *Atp7b*$^{-/-}$ mice did not have decreased bile flow (data not shown). *Bsep*-KO animals on a mixed genetic background do not have significant cholestasis, due to decreased hydrophobicity of the bile acid pool and increased alternative basolateral bile acid transport (41, 42). Likewise, *Fxr*$^{-/-}$ mice have increased *Mrp4*, *Cyp3a11*, and *Cyp2b10* mRNA expression levels as well as increased hydroxylated bile acids (43, 44), and *Fxr*$^{-/-}$ animals have increased *Mrp4* mRNA expression levels in a bile duct–ligation model of obstructive cholestasis (45). *Atp7b*$^{-/-}$ mice also have increased *Mrp4* ($P < 0.05$) and *Cyp2b10* mRNA expression levels ($P = 0.0557$; Supplemental Figure 8), which should increase alternative bile acid detoxification pathways.

It is interesting that the residual FXR remained responsive to the synthetic GW4064 treatment, with ligand treatment increasing *Bsep* and *SHP* mRNA expression levels to those of the WT control

animals. This suggests a potential therapeutic benefit for ligand-mediated activation of FXR in patients with WD.

We found that the activity of additional hepatic nuclear receptors was also changed in the *Atp7b*$^{-/-}$ mouse. At 2 months of age, *Cyp8b1* mRNA was significantly decreased, and by 5 months of age, recruitment of LRH-1 and HNF4α to the *Cyp8b1* promoter was decreased. *Cyp7a1* mRNA was not significantly decreased at this earlier time point, but HNF4α binding to the *Cyp7a1* promoter was decreased in these mice at 5 months of age. Other HNF4α target genes not involved in bile acid synthesis or uptake were also decreased (histidine-rich glycoprotein [HRG] and ornithine transcarbamaylase [OTC]); however, *Apoc3* mRNA expression was unchanged (Supplemental Figure 9). This supports a role for copper disruption of HNF4α activity, as shown in HepG2 cells (46). In contrast with FXR:RXR, binding of LRH-1 and HNF4α was not significantly changed in these mice until 5 months of age. The transcriptional regulation of *Cyp7a1* and *Cyp8b1* by nuclear receptors has complex compensatory mechanisms (12, 47). The FXR/SHP signaling axis is a well-known repressor of CYP7a1 via SHP recruitment of corepressor complexes at LRH-1–binding elements (47), and an early decrease in SHP expression may maintain expression of *CYP7a1* and other LRH-1 and HNF4α target genes.

A straightforward interpretation of the in vitro and *Atp7b*$^{-/-}$ mouse results is that copper directly decreases nuclear receptor function by competing with zinc for occupancy of the DNA-binding domain. However, such direct binding to nuclear receptors in vivo remains to be established, and other mechanisms may also contribute. In cholestatic mouse models such as bile duct ligation, decreased nuclear receptor activity has been attributed to inflammation that resulted in decreased nuclear receptor expression (43, 44, 48, 49). Activation of hepatic stellate cells and inflammatory pathways have been specifically associated with decreased RXR expression (21–25). In accord with this, we observed decreased expression of *Rxr* mRNA in the *Atp7b*$^{-/-}$ livers and in the pediatric WD/no trientine and PFIC samples, but not in the adult patient samples. It is likely that decreased RXR function contributes to the decreased activity of FXR and its other heterodimer partners, but not to the observed effects on HNF4α homodimers and LRH-1 monomers.

Oral zinc administration is a therapy used to treat WD (26, 27, 29). The mechanism of zinc action is thought to compete with copper for intestinal absorption and induction of the metal chelator metallothionein (26, 27, 31). In agreement with previous in vitro studies with ERα (7), we found that increased zinc levels could counteract the impact of copper on specific DNA binding with in vitro binding assays and HepG2 cells. Administration of a zinc-enriched diet to *Atp7b*$^{-/-}$ mice reversed the decreased nuclear receptor activity found in KO animals fed a standard chow diet. FXR:RXR target gene mRNA expression recovered to WT levels due to increased *Rxr* mRNA expression and FXR:RXR binding to FXRE response elements. In contrast with the in vitro studies, increased RXR expression was observed in KO animals supplemented with zinc. In a mouse model of alcohol-induced steatosis, zinc supplementation restored HNF4α and PPARα binding to response elements in EMSA assays, and this coincided with decreased expression of oxidative stress markers (50). No changes in superoxide dismutase (*Sod*) mRNA expression (data not shown) were observed in the *Atp7b*$^{-/-}$ or zinc-supplemented *Atp7b*$^{-/-}$ groups relative to WT mice, but zinc-mediated downregulation of copper-mediated redox stress could potentially protect cysteine residues in the nuclear receptor zinc finger from oxidation, in addition to competing with copper for incorporation into the DNA-binding domain.

Alterations in hepatic nuclear receptor target genes in humans were similar to those in the *Atp7b*$^{-/-}$ mice. In the adult WD group, only 1 of the 3 patients had significantly elevated hepatic copper concentrations, which could reflect effective chelation therapy in those patients, even though the individual with elevated copper was the only one listed as being treated with trientine. Because of this unexpected finding, we measured the expression of fibrogenic markers and found elevated *COL1A1* and *TIMP1* mRNA expression levels in all of the WD patients relative to levels in the nondiseased controls. As expected from the *Atp7b*$^{-/-}$ results, the high Cu individual had the lowest *BSEP* and *SHP* mRNA expression levels and decreased binding of FXR, RXR, and LRH-1 to the *BSEP* and *SHP* promoters. *CYP7a1* and *CYP8b1* mRNA expression in the high Cu samples overlapped that of the other groups, and recruitment of LRH-1 and HNF4α was unchanged, which may reflect loss of SHP-mediated repression of CYP7a1 and CYP8b1. The contrast in LRH-1 recruitment to the *BSEP* and *SHP* promoters versus the *CYP7a1* and *CYP8b1* promoters may be due to cooperative overlapping between HNF4α and LRH-1 binding in the *CYP7a1* and *CYP8b1* promoters (12, 14, 51, 52). OTC and *APOC3* mRNA expression levels were decreased in WD patients with high Cu (Supplemental Figure 9), indicating effects on other HNF4α targets.

We also obtained 2 pediatric WD liver biopsy samples, along with records regarding disease state and drug therapy. One newly diagnosed patient had not received chelation therapy (WD/no trientine), and the other patient had received chelation therapy (WD/trientine). Both the adult patient with elevated hepatic copper and the WD/no trientine patient had decreased mRNA expression of *BSEP*, *SHP*, and *NTCP*, whereas the patient with controlled WD (WD/trientine patient) had mRNA expression of nuclear receptor target genes that more closely overlapped that of the control group.

A group of PFIC3 patients was recently described as having hepatic copper levels similar to those of WD patients (19), and we extended those studies to a set of PFIC3 and PFIC2 samples. Two PFIC3 patients were identified as having elevated hepatic copper levels (patient A: 1,136 μg/g liver dry weight; patient B had significant rhodanine-copper histological staining), and PFIC3 patient A had decreased nuclear receptor and target gene mRNA expression, whereas PFIC3 patient B had mRNA expression patterns similar to those of the control pediatric samples. We also obtained liver biopsy samples from 2 PFIC2 patients: patient A (hepatic copper 177 μg/g liver dry weight) and patient B (hepatic copper content not available). Both PFIC2 patients had mRNA expression levels of *BSEP*, *SHP*, and *NTCP* that were in the range of those detected in the WD/no trientine pediatric patient.

Overall, although only a small number of patient samples were available, the trends in nuclear receptor target gene expression and nuclear receptor DNA binding were similar to those observed in the *Apt7b*$^{-/-}$ mice. Thus, we consistently found impaired nuclear receptor binding in both the mouse and adult and pediatric human samples when copper levels were elevated. We conclude that disrup-

tion of nuclear receptor activity presents a new, quite unexpected mechanism that could contribute to the pathology of WD and potentially of other disorders that result in excessive and chronic hepatic copper accumulation. Although we have focused on a subset of nuclear receptors, all nuclear receptors, and potentially other zinc-binding transcription factors, may be affected to a greater or lesser degree. Our results also suggest the restoration of nuclear receptor or other transcription factor function as an additional mechanism for the beneficial effects of zinc supplementation.

Methods

Animal care. Male and female *Atp7b*$^{-/-}$ (C57BLx129S6/SvEv) mice were previously described (5). Animals were given a standard chow diet from Harlan Laboratories. They were provided food and water ad libitum and maintained on a 12-hour light/12-dark cycle and were killed at Zeitgeber time 2–3. For GW4064 (Sigma-Aldrich) treatment, vehicle or GW4064 (50 mg/kg BW) were given by i.p. injection 4 hours before sacrifice (53). For zinc-feeding studies, male and female *Atp7b*$^{+/-}$ mice in mating cages were given either a chow-matched diet or a zinc-enriched chow diet (1,000 ppm; Teklad Diets; Harlan Laboratories). Mice were maintained on the diets after weaning until 2 months of age.

Human specimens. ICP-OES was used to determine the μg/g liver dry weight of adult liver tissue. The pediatric control group consisted of male and female patients (1 with a benign tumor, 1 with developmental tumors, and 1 with Budd-Chiari syndrome) who did not have excessive hepatic copper levels as measured by rhodanine staining. Before beginning chelation therapy and dietary copper restriction, the WD/trientine patient had hepatic copper concentrations of 1,108 μg/g liver dry weight, and the newly diagnosed patient who had not begun treatment (WD/no trientine) had a +4 score of rhodanine staining (+4 indicating the most significant degree of staining). Liver biopsy samples from an additional WD patient (865 μg/g liver dry weight) and from a patient with cirrhosis and cholestasis (727 μg/g liver dry weight) were used for EMSA analysis. PFIC3 patient A had hepatic copper concentrations of 1,136 μg/g liver dry weight, and PFIC3 patient B had a +4 rhodanine score. PFIC2 patient A had hepatic copper levels of 177 μg/g liver dry weight; however, copper data were not available for the PFIC2 patient B.

Cell culture, EMSA, and ChIP analyses. The tissue culture core at Baylor College of Medicine provided HepG2 cells. EMSA analysis was performed with 2 μl FXR and RXR synthesized with the Rabbit Reticulocyte Translation System (Promega) with or without metals (copper sulfate, zinc sulfate, nickel chloride, or cobalt chloride), as indicated in the figure legends, and γ-P^{32}–labeled double-stranded oligonucleotide containing the FXRE on the *BSEP* promoter (18). HepG2 cells treated overnight with DMSO, 75 μM CDCA, 10 μM copper sulfate, and 10–40 μM zinc sulfate and nuclear extracts were harvested (Pierce, Life Technologies), and 5 μg was used for EMSA analysis as described above. Nuclear extracts (5 μg) from HepG2 cells not treated or treated with 10 μM copper sulfate or 10 μM copper sulfate plus 40 μM zinc sulfate were used in the EMSA with γ-P^{32}–labeled double-stranded oligonucleotides containing HNF4α, TR, SP1, GATA, and CREB consensus response elements (Santa Cruz Biotechnology Inc.).

ChIP assays were performed as previously described with the following modifications (54): freshly harvested livers (0.5–1.0 g) were homogenized in PBS containing 1% formaldehyde and incubated at room temperature for 10 minutes; incubation was stopped by the addition of 2.2 M sucrose in 150 mM glycine, 10 mM HEPES (pH 7.6), 15 mM KCl, 2 mM EDTA, 0.15 mM spermine, 0.5 mM spermidine, 0.5 mM DTT, and 1X protease inhibitor cocktail (Roche). The liver homogenate was layered onto a 2.05 M sucrose buffer containing 10% glycerol and 150 mM glycine, 10 mM HEPES (pH 7.6), 15 mM KCl, 2 mM EDTA, 0.15 mM spermine, 0.5 mM spermidine, 0.5 mM DTT, and 1X protease inhibitor cocktail (Roche) and centrifuged at 100,000 *g* for 30 minutes. Purified nuclei (10–50 μg) were sonicated to between 200 and 300 bp and incubated with 10 μg FXR (H-130X), RXR (D-20X), HNF4α (H-171X) antibody (Santa Cruz Biotechnology Inc.), LRH-1 (catalog PP-H2325-10; Perseus Proteomics Inc.), and RNA Pol II (catalog 39097; Cell Signaling Technology) using the Active Motif EZ-ChIP kit. Primers for a gene desert region on chromosome 6 (mouse promoter, catalog 71011; Active Motif) or chromosome 12 (catalog 71001; Active Motif) were used as a negative control. Primers for the mouse and human *CYP7A1* (55), *CYP8B1* (56), *BSEP* (57), and *SHP* (57) were used for real-time PCR analysis of the immunoprecipitated regions.

Human tissue staining. Pediatric liver biopsy samples were stained with rhodanine staining and counterstained with hematoxylin using standard protocols. The degree of copper accumulation was graded according to previously described criteria (58).

Real-time PCR and Western blot analysis. RNA was harvested from approximately 100-mg liver samples in TRIzol reagent (Invitrogen, Life Technologies), and synthesized cDNA (Invitrogen, Life Technologies) was used as a template for real-time PCR with SYBR Green reagent (Roche) on a 384-well LightCycler (Roche). Primers were designed using Roche Universal Primer web-based software. Reactions using mouse cDNA were normalized to 36B4 mRNA expression, and reactions using human cDNA were normalized to 18S mRNA expression.

Western blot analysis was performed with 5 μg nuclear extract or 2 μl FXR plus RXR synthesized with the Rabbit Reticulocyte Translation System using 1:1,000 α-FXR (H-130; catalog sc-13063; Santa Cruz Biotechnology Inc.); RXR (D-20; catalog sc-553; Santa Cruz Biotechnology Inc.); HNF4α (H-171; catalog sc-8987; Santa Cruz Biotechnology Inc.); LRH-1 (catalog PP-H2325-10; Perseus Proteomics Inc.); CYP7A1 (N-17; catalog 14423; Santa Cruz Biotechnology Inc.); BSEP (F-6; catalog sc-74500; Santa Cruz Biotechnology Inc.); COL1A1 (C-18; catalog sc-8784; Santa Cruz Biotechnology Inc.); TIMP1 (catalog H-150; catalog sc-5538; Santa Cruz Biotechnology Inc.); α-SMA (catalog ab15734; Abcam); β-actin (catalog 13E5; Cell Signaling Technology); and histone H3 (catalog 9715; Cell Signaling Technology); or a 1:50,000 secondary antibody.

Serum analysis. Serum was collected ALT and bilirubin levels measured in the Comparative Pathology Laboratory at Baylor College of Medicine. Total serum bile acids were measured with an enzymatic kit (BIOQUANT Image Analysis).

Inductively coupled plasma–optical emission spectroscopy. Liver samples were dried at 60°C for 3 to 4 days to achieve a stable dry weight. Weighed samples were digested using concentrated nitric acid and hydrogen peroxide. Digestates were resuspended in 2% ultra-pure nitric acid (w/w) and analyzed for minerals using ICP-OES (CIROS ICP Model FCE12; Spectro) as previously described (59).

Statistics. Error bars represent the mean ± the SEM. A 2-tailed Student's *t* test was used to compare differences between 2 groups, and a *P* value of less than 0.05 was considered statistically significant.

For multiple group comparisons, 1-way or 2-way ANOVA, followed by either Bonferroni's or Sidak's post-hoc test, were performed, and a *P* value of less than 0.05 was considered statistically significant. All statistical analyses were performed with GraphPad Prism software, versions 5.0 and 6.0 (GraphPad Software).

Study approval. All animal experiments were performed according to NIH guidelines (*Guide for the Care and Use of Laboratory Animals*, 8th ed. The National Academies Press. 2011.), and animal experiments were approved by the IACUC of Baylor College of Medicine.

The IRB of Baylor College of Medicine approved the use of deidentified human tissue from the NDRI (Philadelphia, Pennsylvania, USA) and the Department of Pathology of Texas Children's Hospital (Houston, Texas, USA). Adult male and female human liver biopsy samples were obtained from the NDRI and pediatric samples from the Department of Pathology of Texas Children's Hospital. The protocols for sample use were approved by the IRB of Baylor College of Medicine.

Acknowledgments

This work was supported by grants from the NIH, National Institute of Diabetes and Digestive and Kidney Diseases (NIDDK) (5T32 DK-007664-19, F32-DK-089689-01A1, and DK-56338, to C.R. Wooton-Kee), which support the Texas Medical Center Digestive Diseases Center; an R.P. Doherty, Jr. — Welch Chair in Science grant (Q-0022, to D.D. Moore); and a USDA-ARS through Cooperative Agreement grant (58-6250-6-003, to M.A. Grusak). The contents of this publication do not necessarily reflect the views or policies of the USDA, nor does mention of trade names, commercial products, or organizations imply endorsement by the US Government.

Address correspondence to: David D. Moore, Department of Molecular and Cellular Biology, Baylor College of Medicine, One Baylor Plaza, Houston, Texas 77030, USA. Phone: 713.798.3313; E-mail: moore@bcm.edu.

1. Lutsenko S, Barnes NL, Bartee MY, Dmitriev OY. Function and regulation of human copper-transporting ATPases. *Physiol Rev*. 2007;87(3):1011–1146.
2. Cater MA, La Fontaine S, Shield K, Deal Y, Mercer JF. ATP7B mediates vesicular sequestration of copper: insight into biliary copper excretion. *Gastroenterology*. 2006;130(2):493–506.
3. Schilsky ML, Irani AN, Gorla GR, Volenberg I, Gupta S. Biliary copper excretion capacity in intact animals: correlation between ATP7B function, hepatic mass, and biliary copper excretion. *J Biochem Mol Toxicol*. 2000;14(4):210–214.
4. Buiakova OI, et al. Null mutation of the murine ATP7B (Wilson disease) gene results in intracellular copper accumulation and late-onset hepatic nodular transformation. *Hum Mol Genet*. 1999;8(9):1665–1671.
5. Huster D, et al. Consequences of copper accumulation in the livers of the Atp7b$^{-/-}$ (Wilson disease gene) knockout mice. *Am J Pathol*. 2006;168(2):423–434.
6. Mangelsdorf DJ, et al. The nuclear receptor superfamily: the second decade. *Cell*. 1995;83(6):835–839.
7. Predki PF, Sarkar B. Effect of replacement of "zinc finger" zinc on estrogen receptor DNA interactions. *J Biol Chem*. 1992;267(9):5842–5846.
8. Deegan BJ, et al. Structural and thermodynamic consequences of the replacement of zinc with environmental metals on estrogen receptor alpha-DNA interactions. *J Mol Recognit*. 2011;24(6):1007–1017.
9. Chen W, Owsley E, Yang Y, Stroup D, Chiang JY. Nuclear receptor-mediated repression of human cholesterol 7α-hydroxylase gene transcription by bile acids. *J Lipid Res*. 2001;42(9):1402–1412.
10. Chiang JY. Bile acids: regulation of synthesis. *J Lipid Res*. 2009;50(10):1955–1966.
11. Kim I, et al. Differential regulation of bile acid homeostasis by the farnesoid X receptor in liver and intestine. *J Lipid Res*. 2007;48(12):2664–2672.
12. Kir S, Zhang Y, Gerard RD, Kliewer SA, Mangelsdorf DJ. Nuclear receptors HNF4α and LRH-1 cooperate in regulating Cyp7a1 in vivo. *J Biol Chem*. 2012;287(49):41334–41341.
13. Russell DW. The enzymes, regulation, and genetics of bile acid synthesis. *Annu Rev Biochem*. 2003;72:137–174.
14. Zhang M, Chiang JY. Transcriptional regulation of the human sterol 12α-hydroxylase gene (CYP8B1): roles of heaptocyte nuclear factor 4α in mediating bile acid repression. *J Biol Chem*. 2001;276(45):41690–41699.
15. Kong B, Wang L, Chiang JY, Zhang Y, Klaassen CD, Guo GL. Mechanism of tissue-specific farnesoid X receptor in suppressing the expression of genes in bile-acid synthesis in mice. *Hepatology*. 2012;56(3):1034–1043.
16. Kast HR, et al. Regulation of multidrug resistance-associated protein 2 (ABCC2) by the nuclear receptors pregnane X receptor, farnesoid X-activated receptor, and constitutive androstane receptor. *J Biol Chem*. 2002;277(4):2908–2915.
17. Ananthanarayanan M, Balasubramanian N, Makishima M, Mangelsdorf DJ, Suchy FJ. Human bile salt export pump promoter is transactivated by the farnesoid X receptor/bile acid receptor. *J Biol Chem*. 2001;276(31):28857–28865.
18. Schuetz EG, et al. Disrupted bile acid homeostasis reveals an unexpected interaction among nuclear hormone receptors, transporters, and cytochrome P450. *J Biol Chem*. 2001;276(42):39411–39418.
19. Ramraj R, Finegold MJ, Karpen SJ. Progressive familial intrahepatic cholestasis type 3: overlapping presentation with Wilson disease. *Clin Pediatr (Phila)*. 2012;51(7):689–691.
20. Ozdil B, Cosar A, Akkiz H, Sandikci M, Kece C. New therapeutic option with N-acetylcysteine for primary sclerosing cholangitis: two case reports. *Am J Ther*. 2011;18(3):e71–e74.
21. Ghose R, Zimmerman TL, Thevananther S, Karpen SJ. Endotoxin leads to rapid subcellular re-localization of hepatic RXRα: A novel mechanism for reduced hepatic gene expression in inflammation. *Nucl Recept*. 2004;2(1):4.
22. Li D, Zimmerman TL, Thevananther S, Lee HY, Kurie JM, Karpen SJ. Interleukin-1 β-mediated suppression of RXR:RAR transactivation of the Ntcp promoter is JNK-dependent. *J Biol Chem*. 2002;277(35):31416–31422.
23. Denson LA, Auld KL, Schiek DS, McClure MH, Mangelsdorf DJ, Karpen SJ. Interleukin-1β suppresses retinoid transactivation of two hepatic transporter genes involved in bile formation. *J Biol Chem*. 2000;275(12):8835–8843.
24. Geier A, Wagner M, Dietrich CG, Trauner M. Principles of hepatic organic anion transporter regulation during cholestasis, inflammation and liver regeneration. *Biochim Biophys Acta*. 2007;1773(3):283–308.
25. Wagner M, et al. Hepatobiliary transporter expression in intercellular adhesion molecule 1 knockout and Fas receptor-deficient mice after common bile duct ligation is independent of the degree of inflammation and oxidative stress. *Drug Metab Dispos*. 2007;35(9):1694–1699.
26. Brewer GJ. Treatment of Wilson's disease with zinc. *J Lab Clin Med*. 1999;134(3):322–324.
27. Brewer GJ, Hill GM, Prasad AS, Rabbani P. Zinc treatment of Wilson's disease. *Ann Intern Med*. 1984;101(1):144–145.
28. Hoogenraad TU. Effective treatment of Wilson's disease with oral zinc. *Arch Neurol*. 1982;39(10):672.
29. Hoogenraad TU, Van den Hamer CJ, Koevoet R, Korver EG. Oral zinc in Wilson's disease. *Lancet*. 1978;2(8102):1262.
30. Hoogenraad TU, Van Hattum J, Van den Hamer CJ. Management of Wilson's disease with zinc sulphate. Experience in a series of 27 patients. *J Neurol Sci*. 1987;77(2–3):137–146.
31. Brewer GJ. Zinc therapy induction of intestinal metallothionein in Wilson's disease. *Am J Gastroenterol*. 1999;94(2):301–302.
32. Frommer DJ. Defective biliary excretion of copper in Wilson's disease. *Gut*. 1974;15(2):125–129.
33. Lewis KO. The nature of the copper complexes in bile their relationship to the absorption excretion of copper in normal subjects in Wilson's disease. *Gut*. 1973;14(3):221–232.
34. Cowen AE, Korman MG, Hofmann AF, Goldstein NP. Biliary bile acid composition in Wilson's disease. *Mayo Clin Proc*. 1975;50(5):229–233.
35. Carpino G, et al. α-SMA expression in hepatic stellate cells and quantitative analysis of hepatic fibrosis in cirrhosis and in recurrent chronic hepatitis after liver transplantation. *Dig Liver Dis*. 2005;37(5):349–356.
36. Berkowitz CM, Shen CS, Bilir BM, Guibert E,

Gumucio JJ. Different hepatocytes express the cholesterol 7α-hydroxylase gene during its circadian modulation in vivo. *Hepatology*. 1995;21(6):1658–1667.
37. Stroeve JH, Brufau G, Stellaard F, Gonzalez FJ, Staels B, Kuipers F. Intestinal FXR-mediated FGF15 production contributes to diurnal control of hepatic bile acid synthesis in mice. *Lab Invest*. 2010;90(10):1457–1467.
38. Song KH, Li T, Owsley E, Chiang JY. A putative role of micro RNA in regulation of cholesterol 7α-hydroxylase expression in human hepatocytes. *J Lipid Res*. 2010;51(8):2223–2233.
39. Hutchens TW, Allen MH, Li CM, Yip TT. Occupancy of a C2-C2 type 'zinc-finger' protein domain by copper. Direct observation by electrospray ionization mass spectrometry. *FEBS Lett*. 1992;309(2):170–174.
40. Huster D, et al. High copper selectively alters lipid metabolism and cell cycle machinery in the mouse model of Wilson disease. *J Biol Chem*. 2007;282(11):8343–8355.
41. Wang R, et al. Severe cholestasis induced by cholic acid feeding in knockout mice of sister of P-glycoprotein. *Hepatology*. 2003;38(6):1489–1499.
42. Lam P, Wang R, Ling V. Bile acid transport in sister of P-glycoprotein (ABCB11) knockout mice. *Biochemistry*. 2005;44(37):12598–12605.
43. Marschall HU, et al. Fxr(–/–) mice adapt to biliary obstruction by enhanced phase I detoxification and renal elimination of bile acids. *J Lipid Res*. 2006;47(3):582–592.
44. Zollner G, et al. Coordinated induction of bile acid detoxification and alternative elimination in mice: role of FXR-regulated organic solute transporter-α/β in the adaptive response to bile acids. *Am J Physiol Gastrointest Liver Physiol*. 2006;290(5):G923–G932.
45. Stedman C, et al. Benefit of farnesoid X receptor inhibition in obstructive cholestasis. *Proc Natl Acad Sci U S A*. 2006;103(30):11323–11328.
46. Song MO, Freedman JH. Role of hepatocyte nuclear factor 4α in controlling copper-responsive transcription. *Biochim Biophys Acta*. 2011;1813(1):102–108.
47. Goodwin B, et al. A regulatory cascade of the nuclear receptors FXR, SHP-1, and LRH-1 represses bile acid biosynthesis. *Mol Cell*. 2000;6(3):517–526.
48. Trauner M, Arrese M, Lee H, Boyer JL, Karpen SJ. Endotoxin downregulates rat hepatic ntcp gene expression via decreased activity of critical transcription factors. *J Clin Invest*. 1998;101(10):2092–2100.
49. Wagner M, Trauner M. Transcriptional regulation of hepatobiliary transport systems in health and disease: implications for a rationale approach to the treatment of intrahepatic cholestasis. *Ann Hepatol*. 2005;4(2):77–99.
50. Kang X, et al. Zinc supplementation reverses alcohol-induced steatosis in mice through reactivating hepatocyte nuclear factor-4α and peroxisome proliferator-activated receptor-α. *Hepatology*. 2009;50(4):1241–1250.
51. Eloranta JJ, Kullak-Ublick GA. Coordinate transcriptional regulation of bile acid homeostasis and drug metabolism. *Arch Biochem Biophys*. 2005;433(2):397–412.
52. Yang Y, Zhang M, Eggertsen G, Chiang JY. On the mechanism of bile acid inhibition of rat sterol 12α-hydroxylase gene (CYP8B1) transcription: roles of α-fetoprotein transcription factor and hepatocyte nuclear factor 4α. *Biochim Biophys Acta*. 2002;1583(1):63–73.
53. Schmidt DR, et al. AKR1B7 is induced by the farnesoid X receptor and metabolizes bile acids. *J Biol Chem*. 2011;286(4):2425–2432.
54. Ripperger JA, Schibler U. Rhythmic CLOCK-BMAL1 binding to multiple E-box motifs drives circadian Dbp transcription and chromatin transitions. *Nat Genet*. 2006;38(3):369–374.
55. Shin DJ, Osborne TF. Peroxisome proliferator-activated receptor-γ coactivator-1α activation of CYP7A1 during food restriction and diabetes is still inhibited by small heterodimer partner. *J Biol Chem*. 2008;283(22):15089–15096.
56. del Castillo-Olivares A, Campos JA, Pandak WM, Gil G. The role of α1-fetoprotein transcription factor/LRH-1 in bile acid biosynthesis: a known nuclear receptor activator that can act as a suppressor of bile acid biosynthesis. *J Biol Chem*. 2004;279(16):16813–16821.
57. Ananthanarayanan M, et al. Histone H3K4 trimethylation by MLL3 as part of ASCOM complex is critical for NR activation of bile acid transporter genes and is downregulated in cholestasis. *Am J Physiol Gastrointest Liver Physiol*. 2011;300(5):G771–G781.
58. Ludwig J, McDonald GS, Dickson ER, Elveback LR, McCall JT. Copper stains and the syndrome of primary biliary cirrhosis. Evaluation of staining methods and their usefulness for diagnosis and trials of penicillamine treatment. *Arch Pathol Lab Med*. 1979;103(9):467–470.
59. Farnham MW, Keinath AP, Grusak MA. Mineral concentration of broccoli florets in relation to year of cultivar release. *Crop Sci*. 2011;51(6):2721–2727.